CrossMark

Effect of solvents on sol–gel spin-coated nanostructured Al-doped ZnO thin films: a film for key optoelectronic applications

K. Deva Arun Kumar[1] · S. Valanarasu[1] · A. Kathalingam[2] · V. Ganesh[3] · Mohd. Shkir[3] · S. AlFaify[3]

Abstract

Aluminum-doped zinc oxide (AZO) thin films were deposited by sol–gel spin coating technique onto the glass substrates using different solvents such as 2-methoxyethanol, methanol, ethanol and isopropanol. Prepared films were characterized by XRD, Raman spectrum, SEM, UV–visible spectrophotometer, photoluminescence (PL) and electrical studies. XRD studies showed that all the prepared films are hexagonal wurtzite structure with polycrystalline nature oriented along (002) direction. SEM images showed uniform particles of size around 60 nm distributed regularly on to the entire glass substrate. EDX analysis confirmed the composition of grown AZO film consisting of Al, Zn and O elements. The prepared films showed highest optical transmittance ~94% in the visible range and band gap 3.30 eV. PL spectra for all AZO films showed a strong UV emission peak at 387 nm. The AZO films prepared using isopropanol solvent showed high carrier concentration and low resistivity values as 1.72×10^{20} cm^{-3} and 2.90×10^{-3} Ω cm, respectively, with high figure of merit (ϕ) value 8.42×10^{-3} (Ω/sq)$^{-1}$.

1 Introduction

Currently, transition-metal oxides and their alloys have been remarkable due to their current chemical and physical properties. ZnO is one of the significant metal oxide materials. ZnO is a multipurpose transparent conducting oxide (TCO) with extraordinary transparency and conductivity perfectly suitable for display device applications [1, 2]. Further, ZnO has high crystallinity, high thermal stability and good mechanical strength, which is suitable to use as electronic material in different fields such as light-emitting diode [3],

(UV) detector [4], solar cell [5] and chemical and gas sensor [6].

It is a group II–VI semiconductor with extensive E_g of (3.36 eV); also it has huge exciton binding energy of 60 meV [7]. ITO is one of the highest used TCO materials; however, indium material is limited and high cost. Instead, doped ZnO is good alternate for ITO in many applications, because it is low cost, nontoxic and high thermal stability material [8]. Among varius metal doped ZnO, specifically, aluminum-doped zinc oxide (AZO), shows good optical and electrical properties and are easily available compared to ITO because of its low cost, which attracts it for large-scale coating applications.

Aluminum-doped zinc oxide thin films can be deposited by many physical and chemical methods. Every deposition method has its own advantages and disadvantages according to their use. In the literature, ZnO thin films fabricated using different deposition approaches, viz. CVD [9], PLD [10], spray pyrolsis [11], RF magnetron sputtering [12], SILAR method [13] and sol–gel [14] are available. Among these, the sol–gel method is a simple method used for the preparation of different metal oxide thin films. In addition to the mild processing conditions, sol–gel method resultant material usually exhibits excellent thermal stability [15]. Further, this method gives many advantages regarding repeatability, reliability, low temperature and composition

✉ Mohd. Shkir
  shkirphysics@gmail.com; shkirphysics@kku.edu.sa

✉ S. AlFaify
  sasaalfaify@hotmail.com

[1] PG and Research Department of Physics, Arul Anandar College, Karumathur, Madurai, India

[2] Millimeter-Wave Innovation Technology Research Center (MINT), Dongguk University, Seoul 100-715, Republic of Korea

[3] Advanced Functional Materials and Optoelectronic Laboratory (AFMOL), Department of Physics, Faculty of Science, King Khalid University, P.O. Box 9004, Abha, Saudi Arabia

control. The structural, optical and electrical properties of AZO are strongly reliant on different precursors, time, temperature and various solvents.

Previous researchers have studied only ZnO thin films using various solvents such as isopropyl alcohol (IPA), ethanol (C_2H_6O), 2-methoxyethanol (2-ME) and methanol (MeOH) by sol–gel method [16]. However, they have discussed only structural and optical properties and not reported the electrical properties. So, our main intention in this current work is to investigate for the first time the effect of four different solvents on structural, morphological, optical and electrical properties of AZO thin films using simple and low-cost sol–gel method. By changing the solvents, significant changes on film crystallization, surface topography, optical transparency and electrical resistivity of AZO thin films are obtained. Highly conducting and transparent AZO films suitable for optoelectronic applications are reported.

2 Experimental details

2.1 Solution preparation

The sol–gel preparation steps used in the present study are as follows:

1. Dissolved 0.15 M of zinc acetate dehydrate ($Zn(CH_3COO)_2 \cdot 2H_2O$) in 20 ml of 2-methoxyethanol, methanol, ethanol and isopropanol separately.
2. Dissolved 3% of aluminum chloride hexahydrate ($AlCl_3 \cdot 6H_2O$) in zinc complex solution.
3. Mixed both solutions together and refluxed for 20 min at 60 °C, under constant magnetic stirring.
4. Stabilizing agent monoethanolamine (MEA) is added drop by drop until MEA and Zn reach a molar ratio of 1:1. Stirred solution continuously at 60 °C for another 2 h until the solution becomes clear and homogeneous.
5. Stirred solution aged at room temperature for 48 h, and finally, the sol–gel solution was ready to process for film preparation.

2.2 Preparation of AZO thin films

The 2.5 cm × 2.5 cm Corning glass substrate was cleaned in detergent and acetone in an ultrasonic bath for 5 min each and then dried using hot air oven for 10 min.

Aluminum-doped ZnO (AZO) precursor solution was prepared by 20 ml of four different solvents, namely 2-methoxyethanol, methanol, ethanol and isopropanol, and is mentioned as samples S1, S2, S3 and S4, respectively. The arranged sol–gel solution was deposited onto cleaned glass substrate at 3000 rpm for 30 s using a spin coating instrument. To remove organic residuals and evaporate the

solvents, the deposited films were preheated at 350 °C for 10 min on a hot plate. This process was repeated seven times to prepare good optical AZO films with desired thickness. Finally, the AZO thin films were annealed 500 °C for 2 h in a muffle furnace. After completing the annealing process, the film was placed at room temperature and got highly transparent (light white and internal multiple color) AZO thin film. The layout diagram of AZO thin film preparation process is shown in Fig. 1.

2.3 Characterization tools

The structural phases and crystallite size of the films were analyzed by Bruker AXS D2 PHASER X-ray diffractometer over a 2θ range of 20° to 90°. The thickness of the prepared film was measured by a stylus profilometer (roughness detector with a stylus Taylor Hobson model). The morphology of
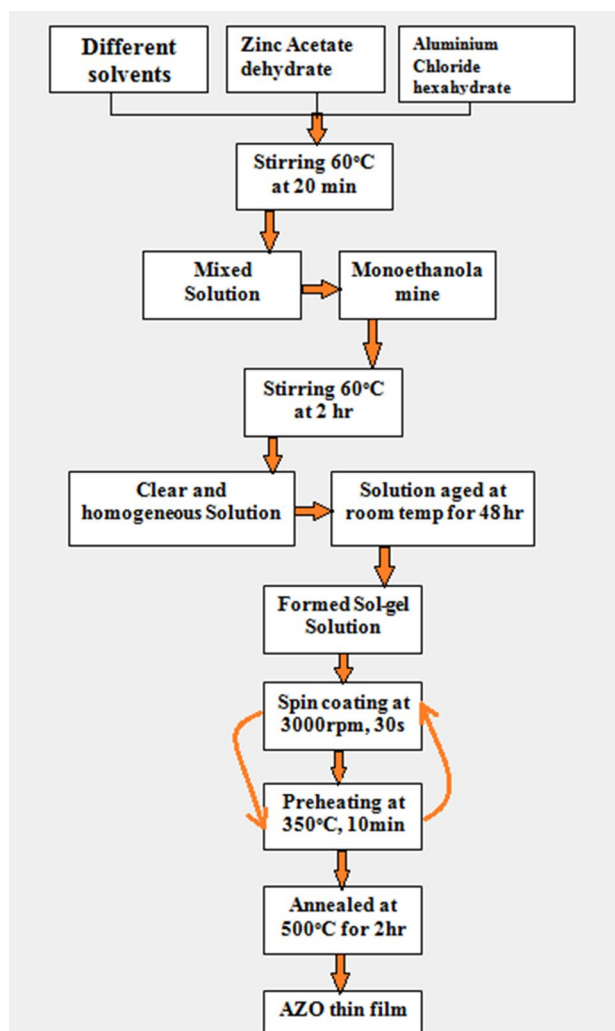

Fig. 1 Process flow chart of the sol–gel spin coating process for the deposited AZO thin films

the AZO films was characterized using SEM (JEOL JSM-6500FE). The chemical composition of the prepared AZO films was studied by EDX. Optical properties of the films were studied using Jasco (V-570) UV–Vis–NIR spectrophotometer. The PL spectra of the AZO films were recorded by spectroflurometer (Jobin Yvon Flurolog-fl3-11) with an excitation wavelength of 325 nm at room temperature. The electrical properties of the AZO films were analyzed by Hall effect measurement by the use of four probe setup.

3 Results and discussion

3.1 Structural properties

Figure 2 shows the X-ray diffraction spectra of AZO films prepared using different solvents such as 2-methoxyethanol, methanol, ethanol and isopropanol which are mentioned as S1,
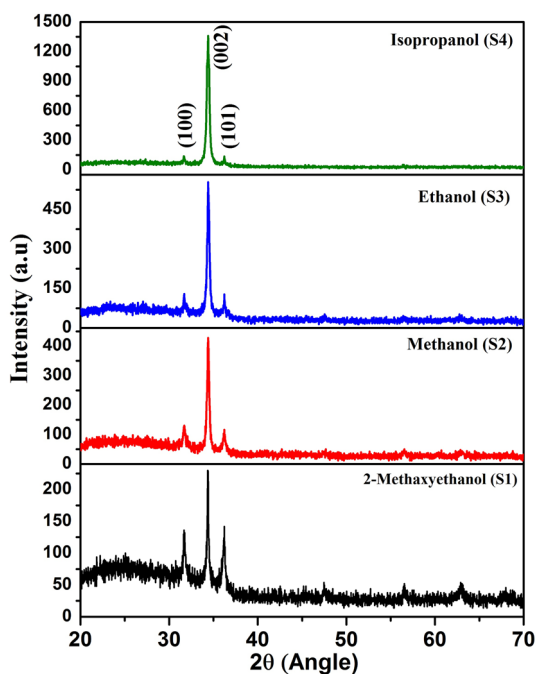

Fig. 2 XRD pattern of AZO thin films with four different solvents such as 2-methoxyethanol (S1), methanol (S2), ethanol (S3) and isopropanol (S4)

S2, S3 and S4 samples. From the XRD studies, the diffraction peaks are observed at 31.72°, 34.46° and 36.19° corresponding to (100), (002) and (101) planes, respectively, for all the films which are belong to a hexagonal structure with polycrystalline nature. All the peaks for the AZO thin films correspond to the standard ZnO structure (JCPDS file no. 79-0205). There are no additional peaks related to aluminum and other alumina phases which indicate that the Al ions are successfully incorporated into ZnO lattice. From XRD figure all the AZO films exhibit the higher intensities of preferential orientation along (002) plane compared to other orientations as (100) and (101). Moreover, the IPA solvent (S4) exhibits the higher preferential orientation compared to other three solvents (S1), (S2) and (S3). This high-intense peak of IPA solvent-used film may be due to the annealing-induced orientation in the preferred (002) plane [17]. A similar phenomenon has already been reported for IPA solvent [18]. A solvent corresponding change in all the peaks is observed. In general, the increasing peak intensity is the indication of enhancement of film crystallinity.

Crystallite size of AZO films was determined by using the Scherer formula. The (002) orientation was used to calculate the crystallite size [19]:

$$D = \frac{0.9\lambda}{\beta \cos \theta}, \tag{1}$$

where D is the crystallite size, λ is the X-ray wavelength ($\lambda = 1.54$ Å), β is the FWHM and θ is the Bragg angle of (002) peak. Table 1 clearly shows that the crystallite size of AZO thin films is increased with the change solvents from (S1) to (S4) due to decrease in FWHM values for these films. From XRD analysis, it is evidently understood that the film (S4) exhibits a high-crystalline eminence when compared with other films because it has high intensity as well as low FWHM values in this work.

The microstrain, dislocation density and number of crystallites per unit volume of the AZO thin films were determined using the following equations [20, 21]:

$$\varepsilon = \frac{\beta \cos \theta}{4}, \tag{2}$$

$$\delta = \frac{1}{D^2}, \tag{3}$$

Table 1 Structural and lattice parameters of AZO thin films

Samples	Crystallite size (nm)	Dislocation density ($\times 10^{15}$) nm^{-2}	Strain ($\times 10^{-3}$ lines^{-2} m^{-4})	Texture coefficient (TC)	Number of crystallites (N)	Lattice constants	
						a (Å)	c (Å)
S2	31	0.986	0.00368	1.66	7.48	3.203	5.148
S2	34	0.843	0.00341	2.24	9.28	3.221	5.168
S3	37	0.726	0.00316	2.38	6.06	3.229	5.173
S4	40	0.598	0.00286	2.69	4.35	3.240	5.182

$$N = \frac{t}{D^3}, \qquad (4)$$

where (β) is FWHM, (D) is the size of crystallites and (t) is the film thickness. The observed values of microstrain, dislocation density, the number of crystallites per unit volume of AZO films are listed in Table 1. From the table, it is showed that there is reduction in the values of (ε), (δ) and (N) for different solvents due to the reduction in the amount of defects of the films. The texture coefficient (TC) values of (002) plane were determined by using the following equation [22]:

$$TC(hkl) = \frac{I(hkl)/I_0(hkl)}{N_r^{-1} \sum I(hkl)/I_0(hkl)}, \qquad (5)$$

where $I_{(hkl)}$ is the observed intensity, $I_{0(hkl)}$ is the JCPDS standard intensity and N is the number of diffraction planes. Texture coefficients (TCs) were calculated using JCPDS file no: 79-0205 for the (100), (002), (101) planes. A film presents TC (hkl) = 1 for randomly oriented crystallites; on the other hand, the TC value is greater than 1 which specifies the plenty of crystallites in that (hkl) plane. The major plane orientation of the film has high TC value. According to the texture coefficient determination, all the AZO films have higher TC values for the (002) direction, which specifies that the films grow especially in the c-axis orientatio.

The lattice constants for the hexagonal structure of AZO thin films with different solvents were determined using Miller indices (hkl) according to the following relations [23]:

$$\frac{1}{d^2} = \frac{4}{3}\left\{ \frac{h^2 + hk + k^2}{a^2} \right\} + \left\{ \frac{l^2}{c^2} \right\}, \qquad (6)$$

where d is the interplaner distance value and (h), (k) and (l) are Miller indices for the particular diffraction plane. The observed lattice constant values such as $a = 3.240$ Å and $c = 5.182$ Å for the film (S4) are in good agreement with the (JCPDS: 79-0205) standard value. Further, the lattice constants a and c are found to increase significantly with change of solvents for the AZO films, which may be due to different strain levels for various solvents. The lattice constants and structural parameters of the spin-coated AZO films are listed in Table 1.

3.2 Raman analysis

Raman scattering measurement is the most powerful technique to study the prepared films crystalline nature in the doped semiconductor material. Also the Raman spectrum can be used to identify the lattice defects.

Figure 3 shows the Raman spectra of the prepared AZO thin films with different solvents in the range of 100–1500 cm^{-1}. For all the films, two predominant Raman modes are observed at 570 and 1093 cm^{-1} with a broad
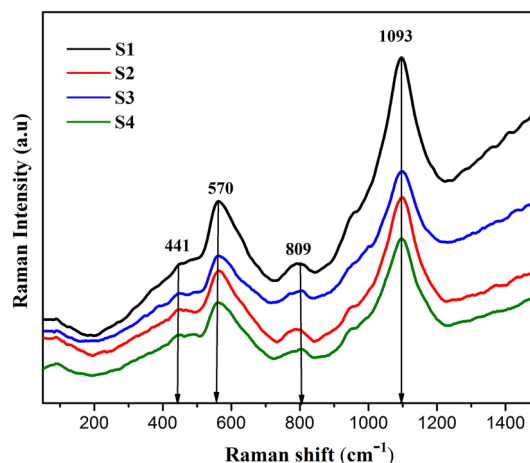

Fig. 3 Raman spectra of AZO thin films of different solvents

peak at 809 cm^{-1}. No other secondary phase like aluminum is identified in all films, because the Al ions are interstitially incorporated into ZnO lattice, and it agrees with our XRD spectrum. The vibration mode observed at 570 cm^{-1} is contributed to both the A$_1$(LO) and E$_1$(LO) modes in all the AZO films. This mode is ascribed to defects of oxygen vacancies and free charge carriers. According to the literature, in this spectral range, there are two-phonon longitudinal A$_1$(LO) modes of ZnO, at 575 and 583 cm^{-1} [24]. Another, A$_1$(TO) mode is observed at 1093 cm^{-1}, and this mode is related to defects like oxygen vacancy, zinc interstitial or their complexes. A broad peak exposed at 809 cm^{-1} is attributed to the glass substrate as a result of the high transmittance in the visible region for AZO thin films. The characteristic 441 cm^{-1} peak of ZnO wurtzite structure, assigned to (E$_2$-high) mode, is present in the Raman spectrum. From the Raman spectrum, same numbers of peaks are observed for different solvents, which confirm the absence of other impurity phases in spite of changing solvents.

3.3 Surface morphology

Figure 4a–d illustrates the SEM images of the AZO thin films coated by spin coating technique with different solvents S1, S2, S3 and S4, respectively. The SEM images confirm that the surface morphology of the films mainly depends on the solvents. No cracks are observed from the film surfaces. The film has a porous nature due to solvent evaporation and dispersion agent during the heating process. The typical grain size of all the AZO is below 100 nm; it confirms that the formed particles are smooth and uniform grains. This property is more useful to enhance the optical and electrical properties of the AZO thin films. Figure 4a shows the structure of excellent particles on the film surface, with grains of size around 45 nm; moreover, this image is
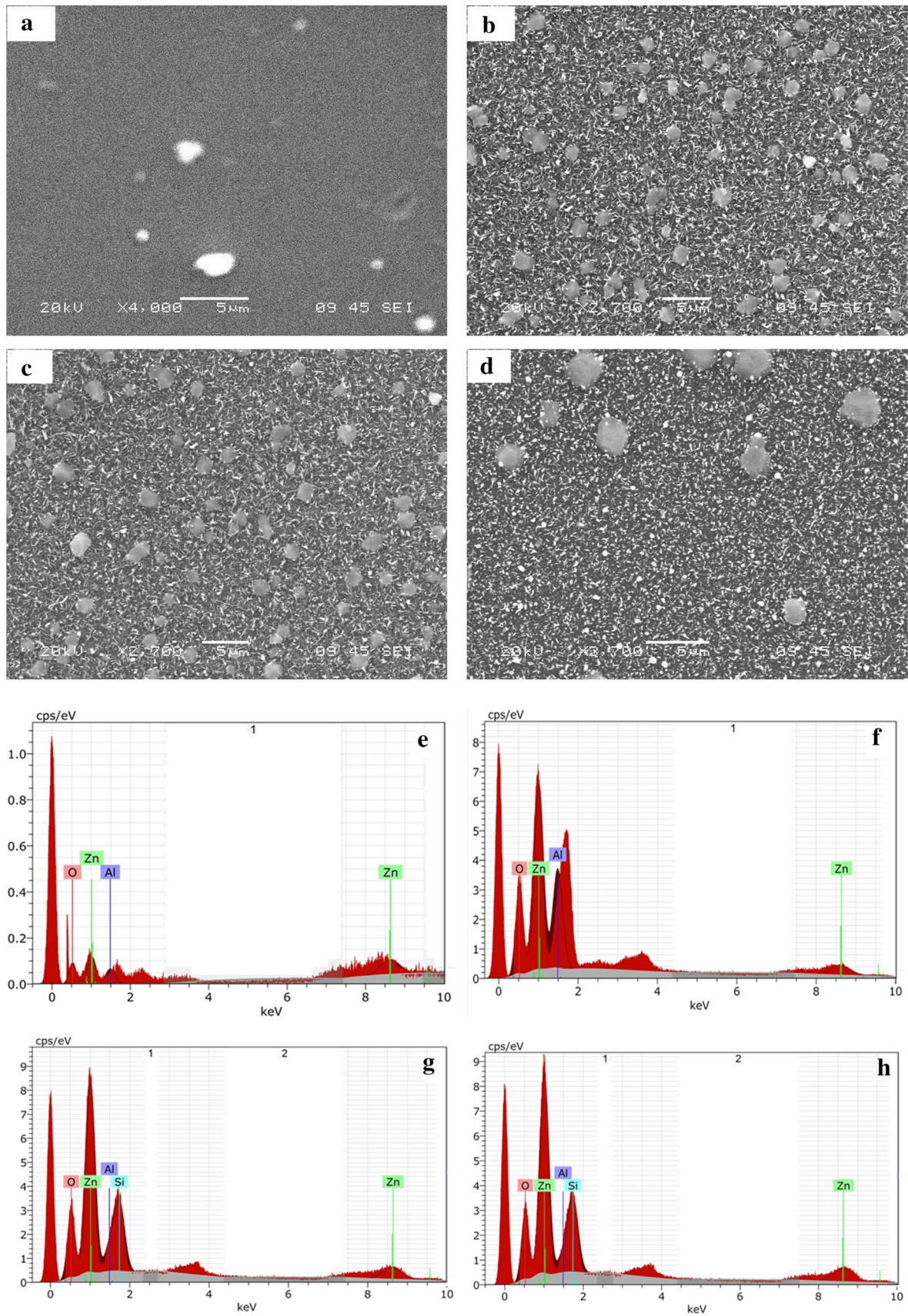
Fig. 4 SEM images of AZO thin films of different solvents **a** S1, **b** S2, **c** S3, **d** S4 and EDAX spectrum of AZO thin films **e** S1, **f** S2, **g** S3, **h** S4

not completely flat and looks crumpled. In Fig. 4b, c, the SEM images show very well nanostructure with the grain size around 60 and 75 nm, respectively. Further, these two images are found to have spherical-shaped particles on entire film surface. Figure 4d clearly shows the excellent particles regularly distributed on to the whole glass substrate, and grain size is 90 nm. These smooth and more spherical-shaped grains with transparent film surface are similar to those reports observed by other researchers [25, 26]. When more grains are presented in the film, there are fewer grain boundaries. Therefore, the atoms are easily moved from one grain to another grain and also the electrical properties are improved. This fact is perfectly matched with the four-point probe results, where the electrical conductivity increased by solvents. The grain size increases with respect to change of solvents this may be due increase of crystallites.

3.3.1 Compositional analysis

In the elemental composition of the prepared AZO thin films, the EDX study was done for all the four films and the result is shown in Fig. 4e–h. In EDX spectrum, our expected peaks of Zn, O and Al are clearly presented showing the growth of AZO thin film. No other impurity peaks are detected in this spectrum, which confirms the pure nature of AZO thin film. The appeared EDX peaks show the atomic ratio of 46.10, 52.35 and 1.55 for Zn, O, and Al, respectively, for the S4 sample. It is exposed that the Al doping ions are successfully incorporated into ZnO lattice.

3.4 Optical properties

The optical transmission is a significant role playing property for transparent conducting oxides (TCO) thin films. The transmittance spectra of AZO with different solvents are presented in Fig. 5, in the wavelength range from 350 to 1100 nm. Generally, the thin film optical transmittance is 65–85% in the visible regions which is high enough for optoelectronic and solar cell applications [27]. The transmittances of all the AZO films are higher than 80% for the entire visible wavelength range with a sharp fundamental absorption edge. From Fig. 5, it is clearly seen that the steep absorbance edge is observed in the UV region of 363–375 nm for all the prepared AZO films, representing the general absorption behavior of thin ZnO films. When the wavelength increased above 350 nm, then absorption suddenly decreased increasing transmittance. Specifically, the 94% transmittance is obtained in the visible region of the film (S1). Our AZO thin films can be used as UV-protected films for optoelectronic devices because these films have less than 40% transmittance in the UV region [28]. In the present study, the average transmittance of all the deposited films varies from 80 to 94% in the wavelength range from
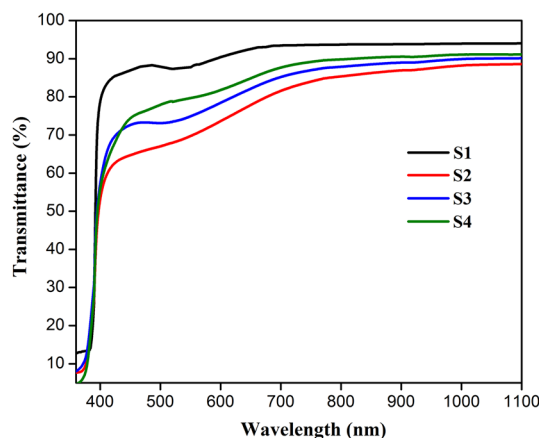
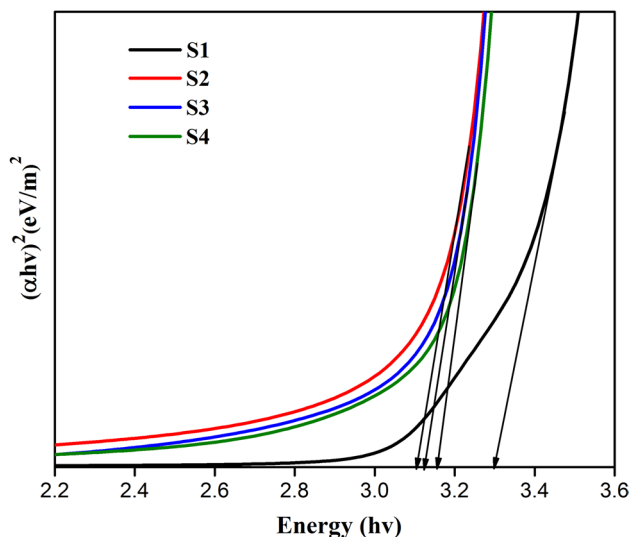**Fig. 5** Optical transmittance of AZO thin films of different solvents

Fig. 6 Relation of $(\alpha h\upsilon)^2$ and $h\upsilon$ of AZO thin films with different solvents

380 to 1100 nm. It is showed that the AZO films can be used as a transparent oxide in solar cells. The optical transmittance initially decreased and then increased with respect to film thickness for changing different solvents. Thickness is the most important tool for film parameter, and it controls the film properties. Thickness measurement of the films (t) was carried out by stylus profilometer. The variation of film thickness with different solvents is listed in Table 2.

The band gap (E_g) was calculated using the following relation [29–31]:

$$\alpha h\upsilon = B(h\upsilon - E_g)^n, \tag{7}$$

where α, h, γ, B and E_g have their usual meanings. Figure 6 shows the obtained band gap of (S1), (S2), (S3) and (S4) AZO thin films as 3.30, 3.11, 3.13 and 3.15 eV, respectively.

The observed band gap of our AZO film is near to the standard Eg value of ZnO (3.36 eV). It is evidence for the formation of ZnO phase. From figure, the sharp absorption edge to be found at 375 nm, which confirms that the prepared ZnO film is a direct band gap semiconductor. The observed band gap value is in good agreement with the previously reported AZO thin films [32].

For optical properties, the refractive index and dielectric constants are the main properties of a TCO material. Refractive index (n) in the wavelength range of 300–1000 nm was calculated from following equation [33]:

$$n = \frac{(1+R)}{(1-R)} + \sqrt{\frac{4R}{(1-R)^2} - k^2}. \tag{8}$$

The graph between refractive index with wavelength range is given in Fig. 7 for AZO films. The refractive index value is in the range of 1.65 to 1.71 at (550 nm) for different solvents (S1–S4) of the AZO thin films. The observed refractive index is in good agreement with the previously reported AZO thin films prepared by other techniques [34].

The extinction coefficient value is calculated using the below relation [35]:

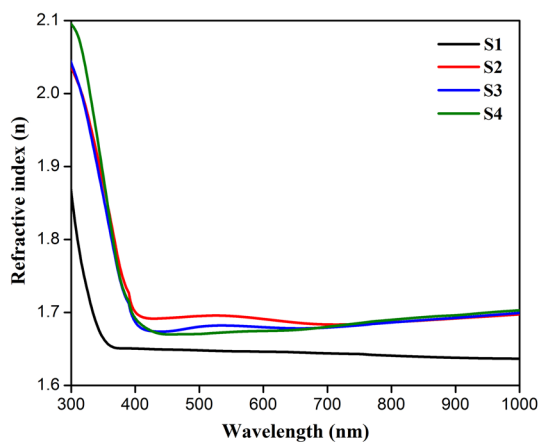$$k = \frac{\alpha \lambda}{4\pi}, \tag{9}$$

Figure 8 shows the spectrum of extinction coefficient (k) versus wavelength. The value of extinction coefficient is low over the entire spectral range which indicates that AZO thin films have the good surface smoothness and high transparency [36]. The obtained (k) values are listed in Table 2, and the variation of extinction coefficient is similar to the variation of refractive index.

Real part (ε_1) and imaginary part (ε_2) of dielectric constants for the AZO thin films were determined from the following relations [37].

$$\varepsilon_1 = n^2 - k^2 \tag{10}$$

$$\varepsilon_2 = 2nk \tag{11}$$

where n is refractive index and k is extinction coefficient. Real part of dielectric constant (ε_1) is related to the speed of light, and imaginary part of dielectric constant (ε_2) is related to the absorption energy from the electric field. The real and imaginary parts of dielectric constants are shown in Figs. 9 and 10, respectively. These figures show that the value of real part (ε_1) is higher than the value of imaginary part (ε_2) of dielectric constant.

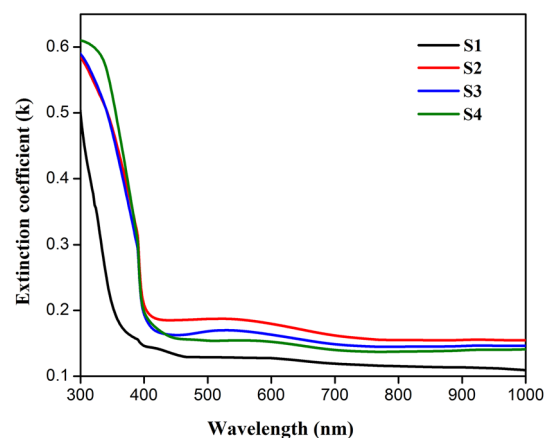Fig. 7 Refractive index of AZO thin films with different solvents

Fig. 8 Extinction coefficient of AZO thin films with different solvents

Table 2 Optical and dielectric parameters of AZO thin films

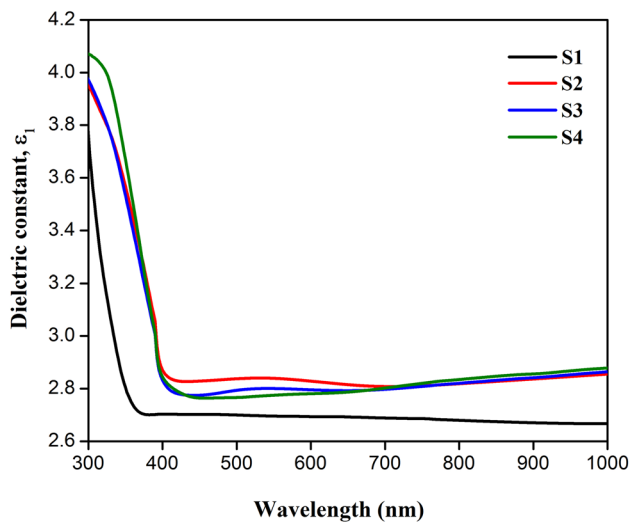| Samples	Transmittance (%)	Thickness (nm)	Band gap (eV)	Refractive index (n)	Extinction coefficient (k)	Dielectric constant (ε_1)	Dielectric constant (ε_2)
S1	94	223	3.30	1.65	0.12	2.70	0.43
S2	80	365	3.11	1.71	0.20	2.85	0.65
S3	84	307	3.13	1.68	0.17	2.80	0.58
S4	87	279	3.15	1.66	0.15	2.77	0.53

Fig. 9 Real part dielectric constant of AZO thin films with different solvents
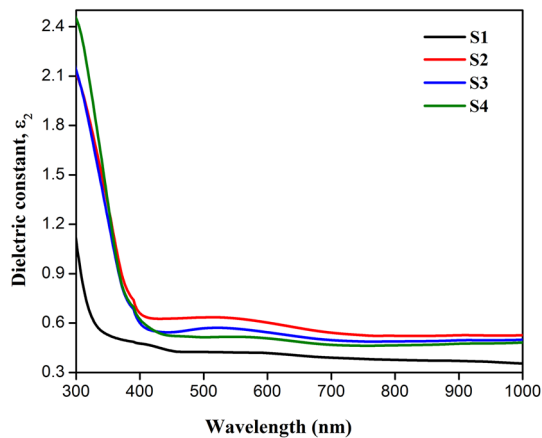

Fig. 10 Imaginary part dielectric constant of AZO thin films with different solvents

3.5 Photoluminescence analysis

Photoluminescence (PL) study also used to analyze the quality of thin films, which depends on film crystallinity, morphology and chemical environment. Usually, ZnO thin films' PL emission spectra exhibit one strong emission peak in the UV region and a broad emission peak in the visible region [38].

The room-temperature PL spectra of the AZO thin films prepared from different solvents are shown in Fig. 11 with a suitable excitation wavelength of 325 nm. The observed PL spectra in all the four films exhibit a strong UV emission peak located at 387 nm and two broad visible emission peaks at 415 and 483 nm. The PL spectra of the AZO films showed UV emission peak at 387 nm is originated from
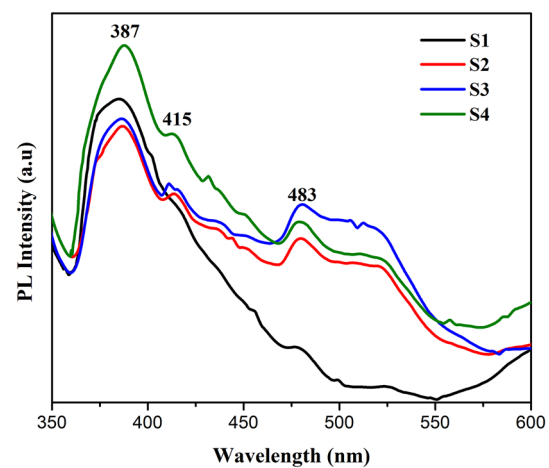

Fig. 11 Photoluminescence spectra of AZO thin films with different solvents

the exciton recombination related to the near-band edge emission (NBE) of ZnO [39]. The (NBE) peak for film (S4) has the strongest UV emission, which is better than that of other films (S1), (S2) and (S3). So, the sharp UV emission peak of S4 films is an indicative of better crystalline quality compared to other three films, and it is in good agreement with our XRD. The two visible emission peaks observed at 415 nm and 483 nm correspond to near blue and blue-green emission, respectively. The near blue emission peak located at 415 nm (2.99 eV) may be attributed to the zinc interstitials (Zn^{2+}) [40]. Broad blue-green emission peak was observed at 483 nm (2.57 eV) due to single ionized oxygen vacancies (V O^+) [41]. Another weak peak of green emission is located at 525 nm (2.36 eV), which may be due to the electron transition from ionized oxygen vacancies to the valence band, it is also reported in the previous work [40]. In the present study, it can be found that the UV emission intensity is high compared to blue emissions for all the AZO films. The observed strong PL (NBE) emission at 387 nm is in good agreement with the previously reported AZO thin film [42]. Compared to other samples, the sample S1 showed poor blue emission at 415 nm and blue–green emission at 483 nm due to the defects such as Zn interstitial and oxygen vacancy, respectively.

3.6 Electrical studies

The electrical properties of sol–gel spin-coated AZO thin films with different solvents were measured by using Hall effect measurement at room temperature. In general, the AZO thin film has high electrical conductivity because of Al^{3+} ions incorporation into the ZnO lattice. Therefore, one free electron is produced in the ZnO lattice when Al^{3+} ions are incorporated. The variation of electrical resistivity,

carrier mobility and carrier concentration of AZO thin films as a function of different solvents is shown in Fig. 12 and listed in Table 3. Here, the electrical properties are mainly depended on the different solvents. From the figure, it is clearly visible that carrier concentration increases with respect to different solvents due to reduction in the grain boundary scattering to free charge carriers and increase in carrier lifetime. In addition, as shown in SEM images (Fig. 4d), the (S4) film has sensibly smoothed and uniform grains over the film surface, so it is the reason for the increase in carrier concentration and reduction in film resistivity (see Fig. 12; Table 3). Another supporting result is that the XRD spectrum also evidences the higher film crystallinity for the (S4) film. From Table 3, the enhanced carrier concentration decreases the carrier mobility by ionized impurity scattering mechanism in the AZO thin films as reported by Shen et al. [43]. The observed high conductivity and low resistivity values are 3.44×10^2 $(\Omega\ \mathrm{cm})^{-1}$ and 2.90×10^{-3} Ω cm, respectively, for the film (S4). We conclude from the electrical studies that the sample S1 is having high electrical resistivity and low carrier concentration, which suggests that 2-methoxyethanol solvent (S1) is worst compared to others.

The figure of merit (ϕ) is acting an important part for optoelectronic applications. A high figure of merit implies a good optical transmittance and a small sheet resistance, hence a better quality of the film. The figure of merit is determined by Haacke's formula [44]:

$$(\varphi) = \frac{T^{10}}{R_{\mathrm{sh}}}, \tag{12}$$

where T is transmittance at a particular wavelength and R_{sh} is sheet resistance. The figure of merit (ϕ) values is presented in Table 3. From this table, it is revealed that the figure of merit (ϕ) initially decreased and then increased with changing different solvents such as (S1), (S2), (S3) and (S4), which may be due to change in the film thickness. As observed, the optical and electrical parameters are acting a key role in deciding the quality of the TCO materials. In general, the transmittance and conductivity must be as high as possible for optoelectronic (TCO) applications [45]. In this report, both the observed transmittance and conductivity values are high, so it can be easily used in optoelectronic applications.

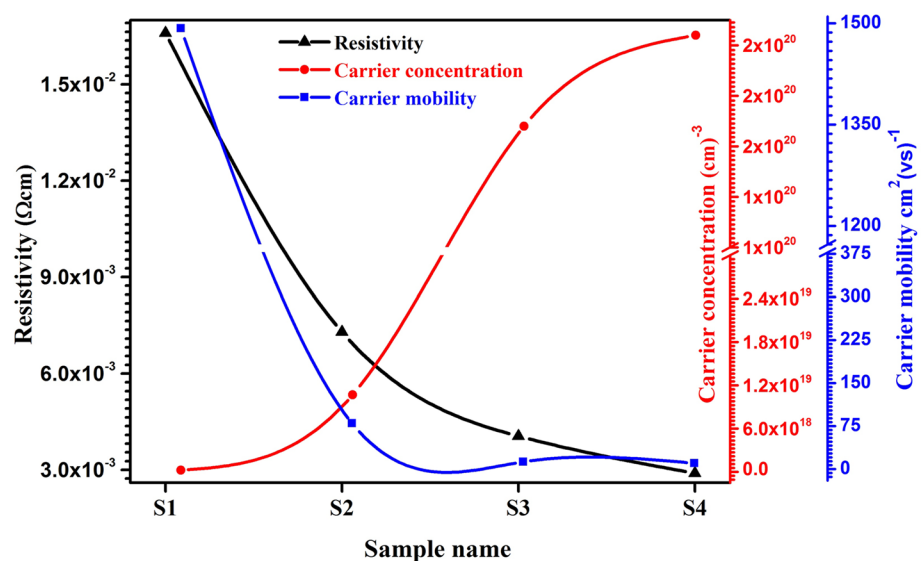**Fig. 12** Variations of electrical resistivity, carrier concentration and carrier mobility of AZO thin films

Table 3 Electrical parameters of AZO thin films with different solvents

Samples	Sheet resistance (Rsh) Ω/sq	Resistivity (ρ) Ω cm	Carrier concentration cm^{-3}	Carrier mobility (μ) $\times$ cm^2 (VS)$^{-1}$	Conductivity (σ) $(\Omega$ cm$)^{-1}$	Figure of merit ϕ 10^{-3} $(\Omega$/sq$)^{-1}$
S1	745	1.66×10^{-2}	2.52×10^{17}	1492.53	6.02×10^1	1.26
S2	200	7.30×10^{-3}	1.07×10^{19}	79.61	1.36×10^2	4.01
S3	132	4.05×10^{-3}	1.54×10^{20}	10.01	2.46×10^2	6.36
S4	104	2.90×10^{-3}	1.72×10^{20}	12.51	3.44×10^2	8.42

In the present work, the obtained electrical resistivity and optical transparency is better than many of the earlier reported values obtained through chemical methods [46–50].

4 Conclusion

Highly transparent conducting aluminum-doped zinc oxide (AZO) thin films were successfully deposited by sol–gel spin coating method onto the glass substrates using different solvents. The prepared films' structural, morphological, optical and electrical properties were mainly depended on the solvents. As from X-ray diffraction (XRD), the doped aluminum ions could be successfully incorporated into pure ZnO wurtzite lattice structure because no aluminum-related peaks were as detected in the AZO films. The (UV–Vis) spectroscopy showed clearly that the 2-methoxyethanol solvent has a good transparency, and the SEM images showed smooth and uniformly covered surface of isopropanol solvent. Among the four different solvents used to produce AZO thin films in this work, isopropanol is established as a best solvent to yield best structural, optical, surface morphological and electrical properties. To the best of our knowledge, for the first time low electrical resistivity and high optical transparency are achieved using different solvents in sol–gel method for AZO film.

Compliance with ethical standards

Conflict of interest Authors declare that there is no conflict of interest in the current article.

References

1. A. Kamalianfar, S.A. Halim, A. Khorsand Zak, Synthesis of ZnO/Cu micro and nanostructures via a vapor phase transport method using different tube systems. Ceram. Int. **40**, 3193–3198 (2014)

2. T.-C. Li, C.-J. Chung, C.-F. Han, J.-F. Lin, Effects of inclination angle applied to a polyethylene terephthalate substrate before the coating of Al-doped ZnO on film quality and mechanical and optical properties. Ceram. Int. **40**, 6987–6998 (2014)

3. H. Guo, J. Zhou, Z. Lin, ZnO nanorod light-emitting diodes fabricated by electrochemical approaches. Electrochem. Commun. **10**(1), 146–150 (2008)

4. G. Chai, O. Lupan, L. Chow, H. Heinrich, Crossed zinc oxide nanorodsfor ultraviolet radiation detection. Sens. Actuators A Phys. **150**(2), 184–187 (2009)

5. E. Guillen, E. Azaceta, L.M. Peter, A. Zukal, R. Tena-Zaera, J.A. Anta, ZnO solar cells with an indoline sensitizer: a comparison between nanoparticulate films and electrodeposited nanowire arrays. Energy Environ. Sci. **4**(9), 3400–3407 (2011)

6. D. Barreca, D. Bekermann, E. Comini, A. Devi, R.A. Fischer, A. Gasparotto, C. Maccato, G. Sberveglieri, E. Tondello, 1D ZnOnano-assemblies by plasma-CVD as chemical sensors for flammable and toxic gases. Sens. Actuators B Chem. **149**(1), 1–7 (2010)

7. A.K. Harish Bahadur, R.K. Srivastava, S.S. Chandra, Morphologies of sol– gel derived thin films of ZnO using different precursor materials and their nanostructures. Nanoscale Res. Lett. **2**, 469–475 (2007)

8. M. Dutta, S. Mridha, D. Basak, Effect of sol concentration on the properties of ZnO thin films prepared by sol–gel technique. Appl. Surf. Sci. **254**, 2743–2747 (2008)

9. W.H. Kim, W.J. Maeng, M.K. Kim, H. Kim, Low pressure chemical vapor deposition of aluminum-doped zinc oxide for transparent conducting electrodes. J. Electrochem. Soc. **158**, D495–D499 (2011)

10. A.C. Galca, M. Secu, A. Vlad, J.D. Pedarnig, Optical properties of zinc oxide thin films doped with aluminum and lithium. Thin Solid Films **518**, 4603–4606 (2010)

11. K. Mahmood, S.B. Park, Atmospheric pressure based electrostatic spray deposition of transparent conductive ZnO and Al-doped ZnO (AZO) thin films: effects of Al doping and annealing treatment. Electron. Mater. Lett. **9**, 161–170 (2013)

12. M.L. Addonizio, A. Antonaia, G. Cantele, C. Privato, Transport mechanism of RF sputtered Al doped ZnO films by H2 process gas dilution. Thin Solid Films **349**, 93–99 (1999)

13. D.J. Edison, W. Nirmala, K.D.A. Kumar, S. Valanarasu, V. Ganesh, M. Shkir, S. AlFaify, Phys. B Condens. Matter **523**, 31–38 (2017)

14. V. Musat, B. Teixeira, E. Fortunato, R.C.C. Monteiro, P. Vilarinho, Al-doped ZnO thin films by sol-gel method. Surf. Coat. Technol. **180–181**, 659–662 (2004)

15. C.J. Brinker, G.W. Scherer, Sol–Gel science. Academic Press, New York (1989)

16. K.L. Foon, M. Kashif, U. Hashim, W.-W. Liu, Effect of different solvents on the structural and optical properties of zinc oxide thin films for optoelectronic applications. Ceram. Int. **40**, 753–761 (2014)

17. N. Shakti, P. Gupta, Structural and optical properties of sol–gel prepared ZnO thin film. Appl. Phys. Res. **2**(1), P19 (2010)

18. S.A. Kamaruddin, Y.C. Kah, K.Y. Ho, M.Z. Sahdan, H. Saim, D. Knipp, Zinc oxide films prepared by sol–gel spin coating technique. Appl. Phys. A **104**(1), 263–268 (2011)

19. M. Wang, K.E. Lee, S.H. Hahn, E.J. Kim, S. Kim, J.S. Chung et al., Optical and photoluminescent properties of sol–gel Al-doped ZnO thin films. Mater. Lett. **61**, 1118–1121 (2007)

20. R. Mariappan, M. Ragavendar, V. Ponnuswamy, Growth and characterization of chemical bath deposited $Cd_{1-X}Zn_XS$ thin films. J. Alloys Compd. **509**, 7337–7343 (2011)

21. Z.R. Khan, M.S. Khan, M. Zulfequar, M.S. Khan, Optical and structural properties of ZnO thin films fabricated by sol–gel method. Mater. Sci. Appl. **2**(05), 340–345 (2011)

22. M.H. Mamat, M.Z. Sahdan, Z. Khusaimi, A.Z. Ahmed, S. Abdulah, M. Rusop, Influence of doping concentration on the aluminum doped zinc oxide thin films properties for ultraviolet photoconductive sensor applications. Opt. Mater. **32**, 696–699 (2010)

23. N. El-Kadry, A. Ashour, S.A. Mahmoud, Structural dependence of dc electrical properties of physically deposited CdTe thin films. Thin Solid Films **269**, 112–116 (1995)

24. C. Bundesmann, N. Ashkenov, M. Schubert, D. Spemann, T. Butz, E.M. Kaidashev, M. Lorenz, M. Grundmann, Raman scattering in ZnO thin films doped with Fe, Sb, Al, Ga, and Li. Appl. Phys. Lett. **83**(10), 1974–1976 (2003)

25. V. Kumari, V. Kumar, B.P. Malik, D. Mohan, R.M. Mehra, Laser induced nonlinear optical properties of zinc oxide thin film prepared. J. Nano Electron. Phys. **3**, 601–609 (2011)

26. M. Saleem, L. Fang, A. Wakeel, M. Rashad, C.Y. Kong, Simple preparation and characterization of nano-crystalline zinc oxide thin films by sol–gel method on glass substrate. World J. Condens. Matter Phys. **2**, 10–15 (2012)

27. K. Deva Arun Kumar, S. Valanarasu, V. Tamilnayagam, L. Amalraj, J. Mater. Sci Mater. Electron. (2017). https://doi.org/10.1007/s10854-017-7278-7

28. Q. Zhang et al., High stable, transparent and conductive ZnO/Ag/ZnO nanofilm electrodes on rigid/flexible substrates. Energies **9**, 443–452 (2016)

29. J. Tauc, R. Grigorovici, A. Vancu, Optical properties and electronic structure of amorphous germanium. Phys. Status Solidi **15**, 627–637 (1966)

30. M. Shkir, I.S. Yahia, V. Ganesh, H. Algarni, S. AlFaify, Facile hydrothermal-assisted synthesis of Gd^{3+} doped $PbI2$ nanostructures and their characterization. Mater. Lett. **176**, 135–138 (2016)

31. M. Shkir, S. AlFaify, I.S. Yahia, M.S. Hamdy, V. Ganesh, H. Algarni, J. Nanopart. Res. **19**, 328–336 (2017)

32. V. Srikant, D.R. Clarke, On the optical band gap of zinc oxide. J. Appl. Phys. **83**, 10–15 (1998)

33. T.S. Moss, *Optical Process in Semiconductor* (Butter worths, London, 1959)

34. N. Baydogan, T. Ozdurmusoglu, H. Cimenoglu, A.B. Tugrul, *Defect and Diffusion Forum*, vol 334–335, pp 290–293 (2013)

35. Z.Z. You, G.J. Hua, Electrical, optical and microstructure properties of transparent conducting GZO thin films deposited by magnetron sputtering. J. Alloys Comp. **530**, 11–17 (2012)

36. K.S. Usha, R. Sivakumar, C. Sanjeeviraja, Optical constant and dispersion energy of NiO thin films prepared by radio frequency magneto sputtering technique. J. Appl. Phys. **114**, 123501–123510 (2013)

37. M.A. Omar, *Elementary Solid State Physics*, Addison-Wesley Publishing Company, Boston, 1993

38. P. Sagar, P.K. Shishodia, R.M. Mehra, H. Okada, A. Wakahara, A. Yoshida, Photoluminescence and absorption in sol–gel-derived ZnO films. J. Lumin. **126**, 800–806 (2007)

39. J. Li, J. Xu, Q. Xu, G. Fang, Preparation and characterization of Al doped ZnO thinfilms by sol–gel process. J. Alloys Compd. **542**, 151–156 (2012)

40. K. Deva Arun Kumar, V. Ganesh, M. Shkir, S. AlFaify, S. Valanarasu, J. Mater. Sci. Mater. Electron. (2017). https://doi.org/10.1007/s10854-017-7985-0

41. N.L. Tarwal, P.R. Jadhav, S.A. Vanalakar, S.S. Kalagi, R.C. Pawar, J.S. Shaikh, S.S. Mali, D.S. Dalavi, P.S. Shinde, P.S. Patil, Photoluminescence of Zinc oxide nanopowder synthesized by a combustion method. Powder Technol. **208**, 185–188 (2011)

42. A. Mahroug, S. Boudjadar, S. Hamrit, L. Guerbous, Structural, optical and photocurrent properties of undoped and Al-doped ZnO thin films deposited by sol–gel spin coating technique. Mater. Lett. **134**, 248–251 (2014)

43. H.L. Shen, H. Zhang, L.F. Lu, F. Jiang, C. Yang, Preparation and properties of AZO thin films on different substrates. Progr. Nat. Sci. Mater. Int. **20**, 44–48 (2010)

44. G. Mavrodiev, M. Gajdardziska, N. Novkovski, Properties of SnO_2: F films prepared on glass substrates by the spraying method. Thin Solid Films **113**, 93–100 (1984)

45. A.R. Babar, P.R. Deshamukh, R.J. Deokate, D. Haranath, C.H. Bhosale, K.Y. Rajpure, Gallium doping in transparent conductive ZnO thin films prepared by chemical spray pyrolysis. J.Phys. D Appl. Phys. **41**, 135 (2008)

46. A. Douayar, H. Bihri, A. Mzerd, Structural, optical and electrical properties of transparent conducting oxide based on Al doped ZnO prepared by spray pyrolysis. Sens. Transducers **27**, 156–160 (2014)

47. W.Y. Zhang, D.K. He, Z.Z. Liu, L.J. Sun, Z.X. Fu, Preparation of transparent conducting Al-doped ZnO thin films by single source chemical vapor deposition. Optoelectron. Adv. Mater. Rapid Commun. **11**, 1651–1654 (2010)

48. A.S. Enigochitra, S. Ponmani, P. Perumal, Effect of aluminium doping on structural, optical and electrical properties of silar prepared ZnO thin films. Int. J. ChemTech Res. **6**(13), 5241–5245 (2014)

49. A. Crossay, S. Buecheler, L. Kranz, J. Perrenoud, C.M. Fella, Spray-deposited Al-doped ZnO transparent contacts for CdTe solar cells. Sol. Energy Mater. Solar Cells **101**, 283–288 (2012)

50. J. Li, J. Xu, Q. Xu, G. Fang, Preparation and characterization of Al doped ZnO thin films by sol–gel process. J. Alloys Compd. **542**, 151–156 (2001)